Transport properties of a weakly ionized cesium plasma*

D. M. Cox,† H. H. Brown, Jr., L. Schumann, F. Murray,‡ and B. Bederson
Department of Physics, New York University, New York, New York 10003
(Received 15 July 1974)

The transverse component (σ_T) of the tensor electric conductivity of a weakly ionized magnetized plasma has been measured under near-thermal equilibrium conditions. Care has been taken to minimize the effects of $\vec{E}\times\vec{B}$ drifts and finite apparatus size. For magnetic fields that are large enough, it is found that the magnetic field dependence of σ_T is $1/B^2$, in agreement with theory. It is also found that the overall density dependence of σ_T agrees with standard conductivity theory. At the highest values of the magnetic field used, the data show some deviation from theoretical predictions which include only electron transport. This deviation is attributed to ion transport, and opens up the possibility of measuring transport properties of the ions alone.

I. INTRODUCTION

We have recently published an article[1] in which the energy loss of a tenuous low-energy ion beam was measured after passage through a plasma in near thermodynamic equilibrium. The plasma was produced by thermal ionization of alkali (cesium) vapor in a hot tantalum container. Such a plasma, which is essentially homogeneous and isotropic, and is in near thermodynamic equilibrium, is well-suited for the study of fundamental plasma problems. In this article we present some results using a similar plasma, but with different geometry, involving the study of dc electric conductivity in a weakly ionized plasma. The main goals of the present work were to study how the conductivity of our plasma depended on density, temperature, and magnetic field (an external field can be applied without affecting the plasma properties). Later papers will explore other aspects of the conductivity problem in more detail, including extension to higher fractional ionization, ac measurements, and stronger magnetic fields.

The transport properties of fully, partially, and weakly ionized plasmas have been the subject of many theoretical studies.[2] The experimental investigations have been exceedingly sparse, mainly owing to the difficulties of creating plasmas whose properties are sufficiently well defined so that meaningful comparison can be made with theory. We have measured the transverse component of the tensor electric conductivity of a weakly ionized cesium plasma as a function of particle density and magnetic field. The effect of the plasma temperature was also studied, although in the present work the temperature dependence is largely attributable to the fractional ionization dependence on temperature. The plasma used was in near-thermal equilibrium with the walls of an isothermal enclosure, was homogeneous, and had no macroscopic electric or magnetic fields other than those externally imposed.

The current carriers for the parameters used are primarily electrons. Even at weak magnetic fields they are tied to the field lines, but collisions with neutral atoms allow their guiding centers to successively hop across the field lines, opposite to the direction of the applied electric field. The effective transport cross section for this process is the momentum transfer cross section.

At higher values of the magnetic field, the electric current will be dominated by ion transport. Deviations of our data from those predicted were actually observed. At higher magnetic fields than those available in this experiment, the ion conductivity could be investigated in detail.

In a uniform magnetic field $\vec{B}$ that points in the z direction, the conductivity tensor σ is defined by the equation

$$\vec{J}=\sigma\cdot\vec{E}, \tag{1}$$

where $\vec{J}$ is the current density, $\vec{E}$ is the electric field, and σ takes the form[3]

$$\sigma=\begin{bmatrix}\sigma_T & -\sigma_H & 0\\ \sigma_H & \sigma_T & 0\\ 0 & 0 & \sigma_L\end{bmatrix}, \tag{2}$$

where σ_T, σ_H, and σ_L are the transverse, Hall, and longitudinal components of the conductivity, respectively. Equation (1) may be written in terms of vectors as

$$\vec{J}=\sigma_T\vec{E}_\perp+\sigma_H(\vec{k}\times\vec{E}_\perp)+\sigma_L\vec{E}_\parallel, \tag{3}$$

where $\vec{E}_\parallel$ and $\vec{E}_\perp$ are the components of $\vec{E}$ parallel and perpendicular to $\vec{B}$ respectively, and $\vec{k}$ is a unit vector in the z direction. Assuming that σ_L is identical to the conductivity in the absence of a magnetic field, Nighan[4] and Roehling[5] have measured this quantity for a partially ionized gas, and Rynn[6] has measured it for a fully ionized gas. The

transverse conductivity σ_T for a weakly ionized plasma, is the object of the present investigation. It has been measured by Mullaney and Dibelius[7] in an experiment possessing a geometry similar to ours, but which may have considerable end effects. It has also been measured by Pikus *et al.*,[8] but in a geometry where the Hall current is shorted by electrodes, rather than being allowed to circulate freely. In both of these investigations, there was no independent check of the neutral density.

II. PLASMA SOURCE AND EXPERIMENTAL GEOMETRY

The weakly ionized cesium plasma is produced by introducing cesium atoms into an almost isothermal box that can be heated up to 1800 K. The degree of ionization is described by the Saha equation,[9]

$$n_e n_i / n_0 = (2\pi m k T/h^2)^{3/2} e^{-e\varphi/kT}, \tag{4}$$

where n_0, n_e, and n_i are the densities of the neutral atoms, electrons, and ions respectively, m is the electron mass, k is Boltzmann's constant, h is Planck's constant, T is the absolute temperature, e is the magnitude of the electronic charge, and φ the ionization potential of the neutral atoms. Other investigators who have constructed equilibrium plasmas similar to ours are Enriques and Magistrelli,[10] and Agnew and Summers.[11] In containers of the size we are considering, almost all the ionization occurs at the walls. The plasma chamber contains several small holes for diagnostics, and the particles make several thousand bounces before escaping. The losses are made up by steadily trickling in a small amount of cesium vapor. The plasma should, therefore, be described by the Saha equation to a good approximation. Except within a few Debye lengths of the wall, $n_e = n_i$ within the body of the plasma, and the distribution functions should be Maxwellian.

The plasma is contained inside an enclosure that is the space between a coaxial tantalum rod and a tantalum cylinder (Fig. 1). The enclosure is capped off by two thin boron nitride (BN_2) disks, and can be heated to 1800 K by radiation emitted by a surrounding heater. A uniform magnetic field, applied parallel to the symmetry axis, is produced by external Helmholtz-like coils. A radial electric field is created by applying a voltage between the rod and the cylinder, and the resulting current is measured. From the voltage, the current, and geometrical factors, σ_T can be calculated. With this configuration, the $\vec{E}\times\vec{B}$ drift of the ionized part of the gas results in an azimuthal circulation, and does not produce density gradients. The electric conductivity of the hot BN_2 is not high enough to short out the plasma, but is high enough to allow a small current to flow. This sets up a radial electric field that exactly matches that in the middle of the plasma region. The BN_2 disks effectively act as guard rings that eliminate fringing fields from the plasma region. Table I contains a summary of the important plasma and geometrical parameters for the present experiment.

III. EXPRESSION FOR σ_T

Consider a homogenous isothermal partially ionized gas in a magnetic field that points in the z direction. We assume that the fractional ionization is low enough so that only electron-neutral and ion-neutral collisions need be taken into account. (From Table I, the electron-atom collision frequency divided by the electron-ion collision frequency has values ranging from 13 to 2×10^4.) A spherical harmonic expansion of the electron distribution function, when inserted into the Boltzmann equation, leads to the following expression[12] for the electron contribution to σ_T, when the electric field is taken to be dc:

$$\sigma_T^e = -\frac{4\pi e^2}{3m}\int_0^\infty \frac{\nu_e w^3}{\nu_e^2+\Omega_e^2}\frac{\partial f_0^e}{\partial w}\,dw, \tag{5}$$

where w is the electron velocity, f_0^e is the isotropic part of the electron velocity distribution, ν_e is the electron-atom collision frequency for momentum transfer, and Ω_e is the electron cyclotron frequency. The electron collision frequency is given by

$$\nu_e = n_0 w Q_{mt}^e, \tag{6}$$

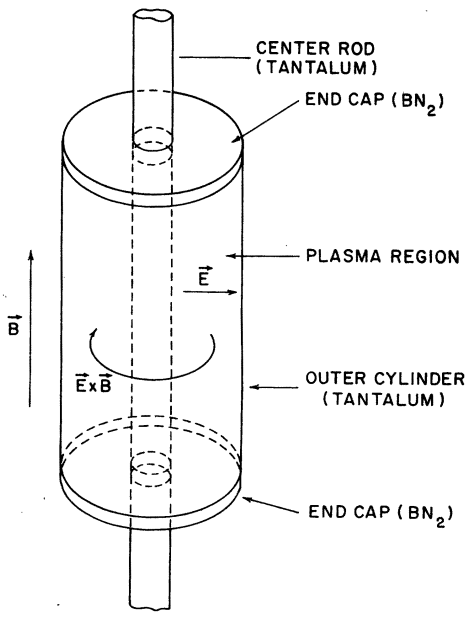

FIG. 1. Schematic diagram of the plasma container.

TABLE I. Summary of plasma and geometric parameters for present experiment.

Temperature	1025–1325 K
Total number density	10^{13}–10^{15} cm^{-3}
Fractional ionization	8×10^{-8}–10^{-4}
Estimated ratio of electron-atom to electron-ion (ν_{90}) collision frequency	13–20,000
Debye length	7×10^{-6}–8×10^{-5} cm
Magnetic field	0.5–225 G
Plasma chamber dimensions	
Inner diameter	0.636 cm
Outer diameter	3.71 cm
Length	20.3 cm

where Q^e_{mt} is the electron-atom cross section for momentum transfer. The ion contribution must be added to this, and indeed, at high magnetic fields will dominate. A corresponding expression for the ion conductivity is

$$\sigma^i_T = -\frac{4\pi e^2}{3\mu}\int_0^\infty \frac{\nu_i W^3}{\nu_i^2+\Omega_i^2}\frac{\partial f_0^i}{\partial W}\,dW, \tag{7}$$

where W is the ion velocity, μ is the reduced ion-atom mass, f_0^i is the isotropic part of the ion velocity distribution, ν_i is the ion-atom collision frequency for momentum transfer, Ω_i is the ion cyclotron frequency, and Q^i_{mt} is the ion-atom cross section for momentum transfer. There may be an addition to ν_i owing to the resonant charge-transfer reaction $Cs^+ + Cs \rightarrow Cs + Cs^+$.

For very weak applied electric fields, it can be shown that f_0^e reduces to the Maxwell-Boltzmann distribution,

$$f_0^e = n_e(\beta_e/\pi)^{3/2}e^{-\beta_e w^2}, \tag{8}$$

where $\beta_e = m/2kT$. We assume that in the same limit f_0^i also approaches the Maxwell-Boltzmann distribution, and

$$f_i^e = n_i(\beta_i/\pi)^{3/2}e^{-\beta_i W^2}, \tag{9}$$

where $\beta_i = M/2kT$ and M is the ion mass. The total conductivity then becomes

$$\sigma_T = \frac{8e^2 n_e \beta_e^{5/2}}{3m\pi^{1/2}}\int_0^\infty \frac{\nu_e w^4}{\nu_e^2+\Omega_e^2}e^{-\beta_e w^2}\,dw + \frac{8e^2 n_i \beta_i^{5/2}}{3\mu\pi^{1/2}}\int_0^\infty \frac{\nu_i W^4}{\nu_i^2+\Omega_i^2}e^{-\beta_i W^2}\,dW. \tag{10}$$

To ascertain the general behavior of σ_T, it is convenient to assume that ν_e and ν_i do not depend on the velocities. This is equivalent to assuming that the cross sections vary as (velocity)$^{-1}$. The integrals in Eq. (10) are then easily evaluated. Figure 2 is a plot of the results for four different neutral densities, $T = 1225$ K, $Q^e_{mt} = (3.11\times10^{-6}/w)$ cm^2 and $Q^i_{mt} = (1.2\times10^{-8}/W)$ cm^2, where w and W are in cm/sec. The constants chosen give conductivities commensurate with those determined from this experiment. For these curves, the arrows pointing down represent the magnetic field values B_e for which $\Omega_e = \nu_e$, and the arrows pointing up represent the magnetic field values B_i for which $\Omega_i = \nu_i$. For $B < B_e$, σ_T is dominated by electron transport and approaches a constant as B is reduced to zero. This is illustrated by the parts of the $n_0 = 10^{14}$ cm^{-3} and $n_0 = 10^{15}$ cm^{-3} curves to the left of the downward arrows. As B gets larger than B_e, as in parts of the above two curves to the right

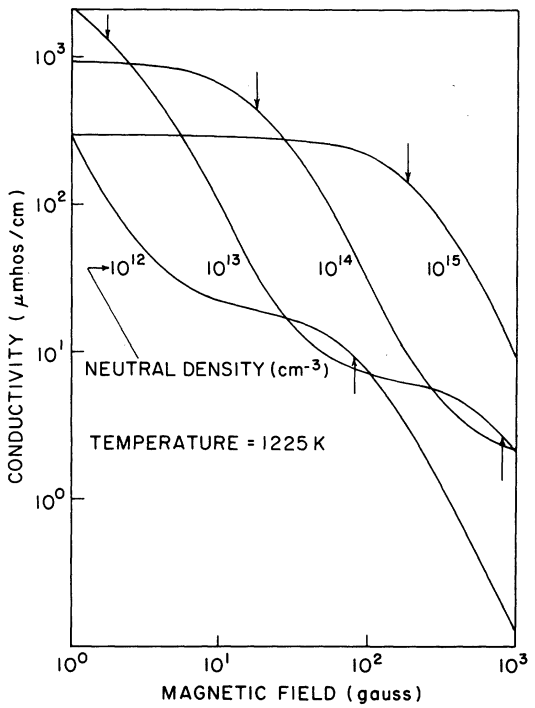

FIG. 2. Calculated values of the transverse conductivity σ_T as a function of magnetic field B, for the four values of the neutral density assuming momentum-transfer electron-neutral (Q^e_{mt}) and ion-neutral (Q^i_{mt}) cross sections of $(3.11\times10^{-6}/w)$ cm^2 and $(1.2\times10^{-8}/W)$ cm^2 respectively, where w and W are the electron and ion speeds. The downward arrows represent fields for which $\Omega_e = \nu_e$.

of the downward arrow, σ_T is still dominated by the electron flow but now has a $1/B^2$ dependence. If electrons were the only charged particles present in the plasma, σ_T would continue to decrease. For ions this is still a low-field region ($\Omega_i \ll \nu_i$) and the ion conductivity is not yet decreasing as $1/B^2$. As B is raised still further, σ_T will level off for a short region with increasing magnetic field until $B > B_i$, where it shows a $1/B^2$ dependence again. In this region the conductivity is almost entirely due to ion transport. This behavior can be seen in the $n_0 = 10^{12}$ cm^{-3} curve to the right of the upward arrow. If one has a large enough magnetic field, it would be possible to investigate the ion conductivity in detail.

In this experiment, the conductivity at zero field is not an accurately measured quantity due to the presence of the sheath resistance. Also, the magnetic field strength is limited and does not allow investigation very far into the region where ion conductivity is important. In the region of primary interest in these measurements $\sigma_T^i \ll \sigma_T^e$, and $\Omega_e \gg \nu_e$. Equation (10) then reduces to

$$\sigma_T \cong \frac{8e^2 n_e \beta_e^{5/2}}{3m\pi^{1/2}\Omega_e^2} \int_0^\infty \nu_e w^4 e^{-\beta_e w^2} dw . \tag{11}$$

Letting $\Omega_e = eB/m$, $\nu_e = n_0 Q_{mt}^e w$, and $\beta_e = m/2kT$, and using Eq. (4) to express n_e in terms of n_0, Eq. (11) becomes

$$\sigma_T = \frac{2^{5/4}\pi^{1/4} m^{17/4} n_0^{3/2} e^{-e\varphi/2kT}}{3h^{3/2}(kT)^{7/4}B^2} \times \int_0^\infty Q_{mt}^e w^5 e^{-mw^2/kT} dw . \tag{12}$$

Equation (12) cannot be reduced further without knowledge of the dependence of Q_{mt}^e on w. For data at a constant temperature, the $1/B^2$ and $n_0^{3/2}$ dependence of σ_T can be tested by assigning a constant to the value of the integral. For data at different temperatures, some assumption has to be made about the velocity dependence of Q_{mt}^e. A convenient assumption which leads to integrals that are easily evaluated is $Q_{mt}^e = C_l/w^l$, where l is an integer and C_l is a constant. Using this expression for Q_{mt}^e in Eq. (12) we have

$$\sigma_T^{(l)} = \frac{2^{5/4}\pi^{1/4} m^{17/4} n_0^{3/2} C_l e^{-e\varphi/2kT}}{3h^{3/2}(kT)^{7/4}B^2} I_{5-l} , \tag{13}$$

where

$$I_p = \int_0^\infty w^p e^{-mw^2/2kT} dw . \tag{14}$$

$\sigma_T^{(l)}$ is the theoretical expression for σ_T obtained by assuming that $Q_{mt}^e = C_l/w^l$, where l is chosen to optimize the theoretical fit to the experimental data. Many transport experiments have assumed such inverse-power cross-section dependences in obtaining cross sections from transport data. However, this is not a justifiable procedure in those cases where the actual velocity dependence of the cross section is more complicated, as it may very well be in the case of electron-cesium in the thermal energy domain.[13] There is some indication that in this region the cross section may go through a strong maximum.

IV. APPARATUS

The plasma chamber, heating element, heat shields, and cesium feed are shown in Fig. 3. These are surrounded by a water-cooled baffle. The vacuum envelope is a stainless-steel cylinder 18 in. in diameter, and 50 in. high, which is pumped by a trapped 10-in. oil diffusion pump. With the plasma chamber at 1400 K, the pressure is 5×10^{-8} torr.

The annular plasma region is 20.3 cm high, and consists of the space between a 0.635-cm-diam. tantalum rod and a 3.71-cm o.d. $\times$ 0.051-cm-wall tantalum cylinder. As previously remarked, the annual region is capped off by two BN_2 disks. The vapor pressure of BN_2 is low enough ($<10^{-9}$ torr) in the temperature range used in this experiment so as not to present any outgassing problems. At the top, the plasma chamber is joined to a rigid 50-Ω coaxial line to enable rf measurements to be made if desired. At the bottom, not shown in Fig. 3, a crude but flexible coaxial line allows the plasma chamber to expand downward upon heating,

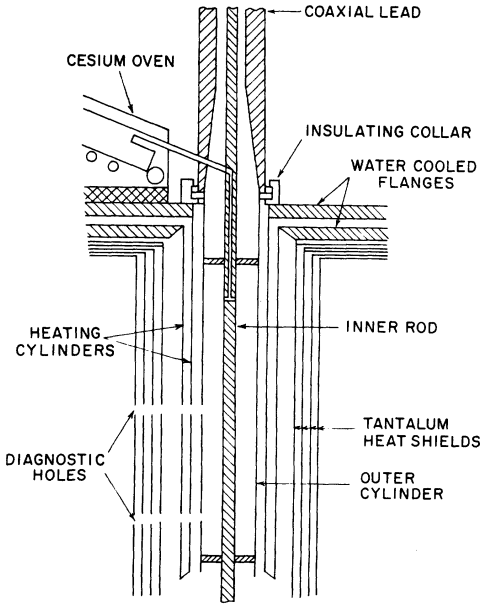

FIG. 3. Cross-sectional view of principal elements of plasma source.

and also permits rf transmission measurements to be made. In addition to having the inner and outer parts of the plasma chamber electrically insulated from each other, the entire assembly is insulated from ground.

The source is similar to many "ovens" used in atomic beam work, except that in addition to heaters, there is a quenching coil through which water or air is passed as needed. Thus, the oven temperature and hence the total particle density is controlled independently of the plasma chamber temperature. The cesium is fed from the oven into the plasma chamber via a hole drilled in the center rod. An Ohmic heater surrounds the plasma chamber, and heats it by radiation. The heating element is constructed from two coaxial tantalum cylinders with 0.001-in. walls welded together at one end. The upper ends of the cylinders are attached to two electrically insulated water-cooled plates. The plates supply the current, which flows down one cylinder and up the other. With this geometry no appreciable magnetic field from the large heating current is created in the plasma region. Similarly, all other current leads both internal and external to the vacuum system are coaxial. About 0.7 kW of filtered dc will heat the plasma chamber to 1200 K. Surrounding the heating element are four cylindrical heat shields fabricated from 0.001-in.-thick tantalum. For diagnostic purposes three small holes are drilled in the plasma chamber, and corresponding holes are cut in the heating element and heat shields. The plasma chamber temperature is measured by sighting into one of these sets of holes with an optical pyrometer. No emissivity corrections are necessary, as the chamber is a very good black body. A correction to the measured temperature is made because of losses in the window of the vacuum system. The neutral density in the plasma chamber is determined by measuring the flux of neutral atoms emanating from one of the holes. A portion of the flux falls on a heated 0.01-in.-diam. tungsten wire and is surface ionized. The resulting ion current is measured, and the neutral density determined from geometrical factors and the plasma temperature. A beam flag is positioned between the hot wire and the exit hole in the plasma chamber so that the neutral background from the hot wire and vacuum chamber could be differentiated from the desired flux emanating from the plasma chamber. Problems arising in the measurement of the neutral flux will be discussed in the next section.

A magnetic field of up to 220 G was supplied by two large Helmholtz-like coils mounted outside the vacuum system. The field was measured with a Bell model 120 gaussmeter. The values obtained were within 3% of those determined by measuring the frequency at which maximum electron cyclotron absorption occurred.

V. EXPERIMENTAL PROCEDURES

A glass capsule of cesium was frozen in liquid nitrogen, cracked, and loaded into the oven. The system was then pumped out as quickly as possible. When the pressure reached ~10^{-7} torr, the plasma chamber heater was slowly turned on so that the temperature of the plasma chamber rose at about 25 K per minute. This prevented the BN_2 insulators from breaking due to thermal shock. After a day or two of outgassing, with the oven kept cold, some measurements were made of the current through the plasma (I) vs the voltage across the plasma (V) in order to determine the resistance of the hot BN_2 end caps. A value of ~7×10^6 Ω was measured, which was independent of the magnetic field. The cesium oven was then heated until the desired density was obtained in the plasma chamber as measured by the hot wire. I-V curves were then taken at very low values of the applied magnetic field, which was vertical, to determine the value at which the vertical component of the earth's field was cancelled. This corresponded to maximum conductivity. The tangential component of the earth's field was ignored. A series of I-V curves were then taken as a function of the magnetic field. σ_T was calculated from the formula

$$\sigma_T = \frac{\ln(b/a)}{2\pi L}\frac{\Delta I}{\Delta V}. \tag{15}$$

$\Delta I/\Delta V$ is the slope of an I-V curve and b, a, and L are the outer radius, the inner radius, and the height of the plasma chamber, respectively. The resistance of the end caps was neglected, as in the worst case it was more than 100 times the resistance of the plasma.

The hot wire signal consists of three parts: alkali ions emitted by the wire, a cesium flux originating from cesium background vapor in the vacuum chamber, and the desired cesium "beam" flux originating from the hole in the plasma chamber. The beam flag, consisting of a rectangular plate 1×1 in., is supposed to separate the last from the first two. The beam flag is swung completely in or out of the beam and the difference in the hot wire signals is recorded. At higher densities, and after the vacuum chamber had not been exposed to air for awhile, the "background" flux in fact became higher than the "beam" flux. Eventually this effect was traced to cesium emitted from the outside of the plasma chamber, near the exit hole. To eliminate this spurious signal, a slit was cut in the middle of the beam flag, and the flag "open" measure-

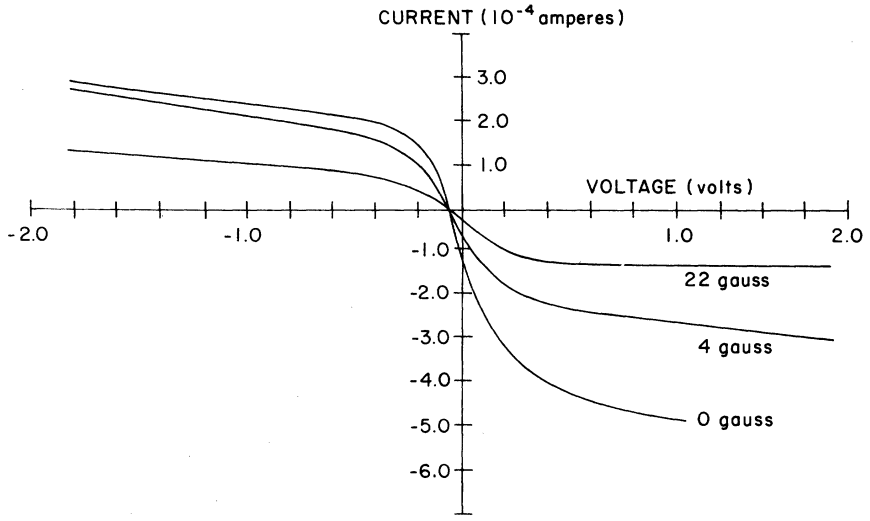

FIG. 4. Some typical overall I-V curves: T = 1300 K; B = 0, 4, and 22 G.

ments were taken through this slit.

As a further qualitative check on the neutral density in the plasma chamber, the transmission rf capabilities of the system were used. An rf signal was fed into the plasma chamber from the top, and detected in the coaxial-cable lead going out the bottom. Choosing the correct value of the plasma frequency as the half-power transmission point, the value of the neutral density predicted from the rf frequency measurement and the Saha equation agreed to within 30% of the hot wire measurements.

All measurements were made with the outer part of the plasma chamber at a fixed potential and with the potential on the inner electrode varied. The I-V curves were then independent of the bias on the outer part, which was usually made zero.

VI. DATA

Figure 4 shows I-V curves for magnetic field values of 0, 4, and 22 G. The magnitude of the maximum voltage applied, 2 V, was very large in the sense that it drove the medium far into a nonlinear region. Positive (negative) voltage means the inner rod is positive (negative) with respect to the outer cylinder. The asymmetry of the saturation values of the curves with respect to plus and minus voltage is probably in part due to the difference in radii of the cylinder and rod. While an investigation of this saturation region would be interesting, for our purposes it was more desirable to keep the applied voltage and collected current as small as practical. In this region of small current flow the I-V curves were found to be very linear, exhibiting none of the saturation characteristics seen at higher voltages. Three such linear I-V curves are shown in Fig. 5 for magnetic fields of 135, 180, and 224 G. The conductivity is obtained from the slope of these curves. The lines do not go through the origin, and the zero intercept changes with the magnetic field. We attribute these effects to thermoelectric voltages generated by the junctions of dissimilar metals, and by thermoelectric effects in the plasma itself.

Careful observation with the optical pyrometer indicated that there was about 10 K temperature difference between the inner rod and outer cylinder. The voltage difference ΔV necessary to produce zero current in the presence of a temperature difference ΔT is

$$\Delta V = \alpha \Delta T / \sigma_T , \tag{16}$$

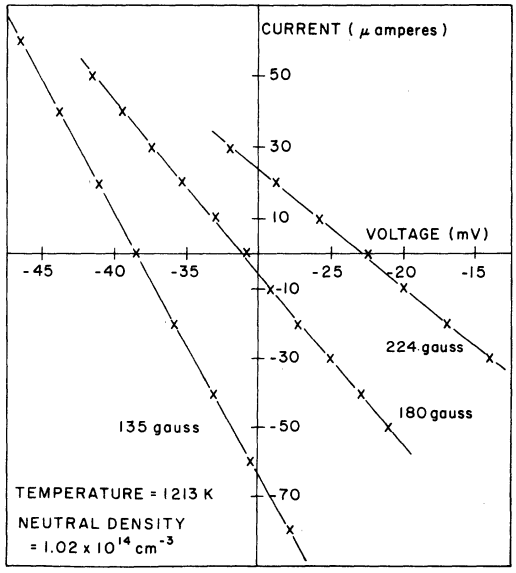

FIG. 5. Some typical I-V curves in linear region: T = 1213 K; B = 135, 180, and 224 G.

where α is the thermoelectric coefficient. From Eastlund's work,[14] we estimate an α (in zero magnetic field) of 10^4 $G^{1/2}K^{-1}sec^{-2}$, and from our own measurements, we estimate a σ_T of 10^{-3} mho/cm at zero magnetic field. With the above values, Eq. (16) predicts 33 mV for 10 K temperature difference, which is the order of magnitude of the zero-current voltage observed. The thermal bias does not significantly affect the conductivity measurements.

Figures 6 and 7 present measured values of the conductivity vs magnetic field. The data are listed in tabular form in Tables II and III. In Fig. 6 there are four sets of data, all taken with $n_0 \cong 10^{14}$ cm^{-3}. The four sets were taken at temperatures of 1021, 1106, 1213, and 1326 K. Because of thermal time constants in the cesium supply and plasma system, it was not practical to experimentally adjust n_0 to be exactly the same in all four cases. The solid straight lines are plots of Eq. (13) with $l=2$ and $C_2 = 59.8$ cm^4. Recall that this expression is valid for $B_e \ll B < B_i$, and predicts a $1/B^2$ dependence of the conductivity on magnetic field. The arrows pointing downward are the values of B_e calculated using the above values of l and C_l. The dotted lines are corrections to Eq. (13) obtained by adding in the ion conductivity as given by Eq. (7) with the assumptions that ν_i is constant and $Q_{mt}^i = 1.2\times10^{-8}/W$ cm^2. For magnetic fields of 30 to 100 G, attempts to fit the data to values $l=0$, 1, 3, or 4 result in worse agreement than with $l=2$.

Table IV contains values of the fractional differences of various $\sigma_T^{(l)}$ from $\sigma_T^{(2)}$ for various temperatures, assuming the density is constant. The C_l are chosen so that the $\sigma_T^{(l)} = \sigma_T^{(2)}$ at 1200 K. These percentage differences are large enough so that $l=2$ is clearly the best value.

In Fig. 7 are five sets of data, all taken at temperatures close to 1225 K. The five sets were taken with $n_0 = 1.2\times10^{13}$, 6.1×10^{13}, 1.3×10^{14}, 4.7×10^{14}, and 1.1×10^{15} cm^{-3}. Again, the solid straight lines are plots of Eq. (13) with $l=2$ and $C_2 = 59.8$ cm^4, and the dotted lines are obtained by adding in the ion conductivity as in Fig. 6. It must be emphasized that in Fig. 7 all the temperatures are quite close together, the integral in Eq. (12) which contains the unknown velocity dependence of Q_{mt}^e is almost a constant, and the temperature variations that do exist are compensated for by an assumed velocity dependence that fits a 325-K temperature variation of the plasma. Figure 7 is hence an excellent test of the $1/B^2$ and $n_0^{3/2}$ predictions of Eq. (12).

We estimate that the measurements of σ_T and B are accurate to ±3%. The temperature, after corrections have been made for window losses, is adjudged known to ±15 K. The relative values of

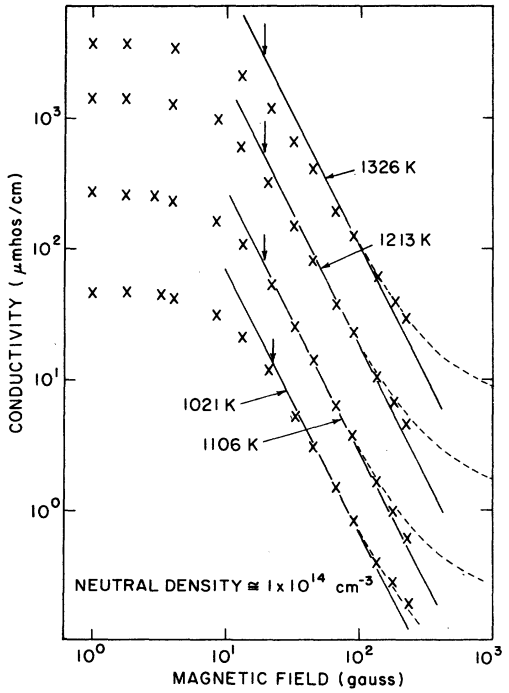

FIG. 6. Measured values of conductivity σ_T vs magnetic field, for a neutral density of about 10^{14} cm^{-3}, for four values of the temperature, as indicated.

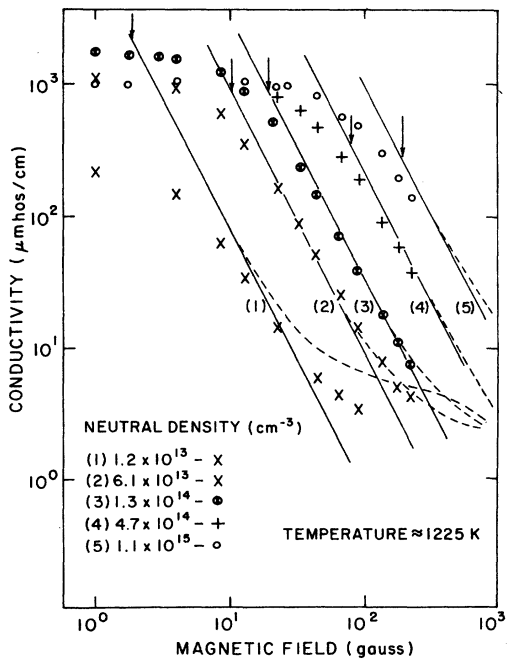

FIG. 7. Measured values of conductivity σ_T vs magnetic field, for a temperature of about 1225 K, at five values of the neutral density, as indicated.

TABLE II. Summary of measured conductivity σ_T vs magnetic field for several temperatures at approximately constant neutral density.

$T=1326$ K, $n_0=1.07\times10^{14}$ cm^{-3}		$T=1213$ K, $n_0=1.0\times10^{14}$ cm^{-3}		$T=1106$ K, $n_0=1.0\times10^{14}$ cm^{-3}		$T=1021$ K, $n_0=1.2\times10^{14}$ cm^{-3}	
σ_T (μmho/cm)	B (G)	σ_T (μmho/cm)	B (G)	σ_T (μmho/cm)	B (G)	σ_T (μmho/cm)	B (G)
3481	0	1404	0	265	0	43.6	0
3351	0.9	1412	0.9	262	0.9	41.9	0.9
3360	1.81	1419	1.8	256	1.79	42	1.8
3126	4.0	1263	4.0	233	4.0	39.3	4.0
1932	13.0	959	8.5	169	8.5	28.9	8.5
1101	22.0	612	13	107	13.0	10.2	21.5
615	33.0	313	22	56	21.5	5.0	33.6
387	44.4	160	32.3	26	32.7	2.7	44.4
188	67	77.6	44.4	14.2	44.4	1.3	67
115	89	37.5	67	6.8	67	0.76	90
58.1	134	22.6	89.1	3.8	89.5	0.38	134
33.0	179	10.3	134	1.7	134	0.26	179
28.0	224	6.6	179	1.0	179	0.18	224
		4.5	224	0.67	224		

the neutral density depend primarily on the measurement of the hot wire current. These relative values are estimated to be accurate to ±4%. The absolute values of the neutral densities are known much less well, primarily because of the large neutral background and uncertainties in dimensions. We assign an uncertainty of ±40% to the absolute values of the neutral densities.

VII. DISCUSSION AND CONCLUSIONS

With respect to the magnitude of the magnetic fields used in this experiment, there are two main regimes of interest. The first is at zero or low values of the field where B has no effect on the conductivity. The second is at higher values of B where the conductivity is essentially falling off as $1/B^2$, but not so high that ion conductivity has become important. In the low-field region it is well known that the resistance of the sheath may be large enough to affect the conductivity measurements of the plasma. Rynn[6] has observed this for a fully ionized plasma, and has developed a theory that does not depend on the details at the surfaces for the order of magnitude of this effect. Extending

TABLE III. Summary of conductivity σ_T vs magnetic field B, for several neutral densities at approximately constant temperature.

$T=1220$ K, $n_0=1.2\times10^{13}$ cm^{-3}		$T=1218$ K, $n_0=6.1\times10^{13}$ cm^{-3}		$T=1228$ K, $n_0=1.3\times10^{14}$ cm^{-3}		$T=1225$ K, $n_0=4.7\times10^{14}$ cm^{-3}		$T=1241$ K, $n_0=1.1\times10^{15}$ cm^{-3}	
σ_T (μmho/cm)	B (G)	σ_T (μmho/cm)	B (G)	σ_T (μmho/cm)	B (G)	σ_T (μmho/cm)	B (G)	σ_T (μmho/cm)	B (G)
225	0	1204	0	1717	0	969	0	1082	0
216	0.9	1002	0.9	1715	0.9	974	13.3	1012	1.8
143	4	928	4	1670	1.8	816	22	1053	4.0
60.1	8.5	594	8.5	1622	2.9	639	33	1015	13
33.3	13	343	13	1564	4.0	477	49.4	955	24
13.6	22.8	158	22.8	1246	8.5	280	67	811	44.4
5.7	45.7	85	32.7	896	13	190	90	541	67
4.1	66	50.6	43.5	510	21.3	91	134	489	89
3.2	90	24	66	236	33.6	57	179	300	134
		13.9	89	149	44.4	36.1	224	200	179
		7.4	134	69	66			140	224
		4.9	179	38.4	90				
		4.1	224	17.4	134				
				10.6	179				
				7.1	224				

TABLE IV. Fractional differences of the $\sigma_T^{(l)}$ from the $\sigma_T^{(2)}$ for various temperatures.

Temperature	1000 K	1100 K	1200 K	1300 K
$(\sigma_T^{(0)}-\sigma_T^{(2)})/\sigma_T^{(2)}$	−0.167	−0.085	0	+0.081
$(\sigma_T^{(1)}-\sigma_T^{(2)})/\sigma_T^{(2)}$	−0.086	−0.045	0	+0.041
$(\sigma_T^{(2)}-\sigma_T^{(2)})/\sigma_T^{(2)}$	0	0	0	0
$(\sigma_T^{(3)}-\sigma_T^{(2)})/\sigma_T^{(2)}$	+0.10	+0.045	0	−0.039
$(\sigma_T^{(4)}-\sigma_T^{(2)})/\sigma_T^{(2)}$	+0.199	+0.090	0	−0.078

Rynn's results for plane parallel geometry to our cylindrical coaxial geometry, we obtain for the sheath resistance R_s

$$R_s=\frac{4}{e^2}\left(\frac{mkT}{3}\right)^{1/2}\frac{A_a+A_b}{A_aA_b}\frac{1}{n_e}, \tag{17}$$

where A_a and A_b are the areas of the inner rod and outer cylinder. When expressed in terms of an equivalent conductivity, Eq. (17) predicts values of the sheath conductivity which are several times higher than that measured but not enough higher to justify neglecting it entirely. Furthermore, an attempt to extend the good theoretical fit to the data at higher values of B down to low values of B resulted in some success, but the results were not good enough to be reproduced here. Even when Eq. (17) was introduced in the theory, there were some discrepancies at one or two values of the density. The obvious way of determining the sheath resistance is to change the radius of the inner rod or outer cylinder of the plasma chamber, which was not feasible in the present experiment.

As B is raised above B_e, the conductivity of the plasma falls rapidly, while that of the sheath should be relatively unaffected, as the cyclotron radius of the electrons is large compared to the sheath dimensions. The agreement between theory and our data as shown in Figs. 6 and 7 is excellent for values of B much above B_e. The one exception to this is the data for $n_0=1.2\times10^{13}$ cm^{-3} in Fig. 7. At this low density the mean free path of the electrons is approaching the dimensions of the chamber and inaccuracies in the theoretical fit are to be expected.

At the highest magnetic fields used, the data deviates slightly from the solid lines. By including in the expression for the theoretical electron conductivity a term representing the conductivity of the ions, better agreement is obtained. Clearly higher magnetic fields than the ones used in this experiment are necessary to investigate the ion conductivity. Such an investigation would be particularly interesting because of the additional effect of charge transfer.

It can be concluded from the excellent agreement between the predictions of Eq. (12) and the data taken near the temperature of 1225 K (Fig. 7) that the $1/B^2$ dependence predicted by Eq. (12) is well satisfied for $B>B_e$. This dependence results from the dynamics of collisions, and the dynamics of charged particles in magnetic fields. Care has been taken in the geometrical design of this experiment to minimize end effects, and $\vec{E}\times\vec{B}$ effects. We believe that this experiment has determined the magnetic field dependence of σ_T to a precision not previously attained.

The $n_0^{3/2}$ dependence of σ_T results from fact that σ_T depends on the densities as n_-n_0. From the Saha equation n_- is seen to be proportional to $n_0^{1/2}$ resulting in a $n_0^{3/2}$ density dependence. The good agreement of the spacing between the five different sets of data in Fig. 7 with the theoretical predictions indicates that both the Saha equation, i.e., near thermodynamic equilibrium, and the basic n_- dependence of σ_T in weakly ionized conductivity theory, obtain in the present experiment.

The data taken at approximately the same density but different temperatures (Fig. 6) indicates that in this temperature range assuming Q_{mt}^e varies as $1/w^2$ produces a better agreement with the data than any other simple power law. Not too much should be read into this, as the velocity dependence of the cross section might be very complicated, with $1/w^2$ just happening to produce the best result. On the other hand, it is interesting to note that a partial-wave expansion of Q_{mt}^e gives[15]

$$Q_{mt}^e=\frac{4\pi\hbar^2}{m^2w^2}\sum_{l=0}^{\infty}(l+1)\sin^2(\eta_l-\eta_{l+1}), \tag{18}$$

where η_l is the phase shift for the lth partial wave. In general the η_l are slowly varying functions of w except near resonances. Thus, far from resonances Q_{mt}^e should vary as $1/w^2$.

Finally, it should be noted that in our experiment the relative values of the neutral density are quite accurate, but the absolute values are not so accurate due to the large neutral background. With apparatus modifications, the absolute neutral density could be measured to much higher precision, and accurate values of the integral containing the momentum transfer cross section obtained.

ACKNOWLEDGMENTS

We gratefully acknowledge the help of Professor T. M. Miller and Dr. I. Klavan throughout the course of this experiment.

*Supported by the National Science Foundation.
†Present address: Esso Research and Eng. Co., Linden, N. J. 07036.
‡Present address: Dept. of Physics, Univ. of Scranton, Scranton, Pa., 18510.

[1]D. M. Cox, H. H. Brown, Jr., I. Klavan, and B. Bederson, Phys. Rev. A 10, 1409 (1974). An earlier version of this work is presented in Phys. Rev. Lett. 28, 1254 (1972).
[2]See references in A. R. Hochstim, *Kinetic Processes in Gases and Plasmas* (Academic, New York, 1969), Chap. VI.
[3]E. H. Holt and R. E. Haskell, *Foundations of Plasma Dynamics* (Macmillan, New York, 1965), Chap. 10.
[4]W. L. Nighan, Phys. Fluids 10, 1085 (1967).
[5]D. Roehling, Adv. Energy Conver. 3, 69 (1963).
[6]N. Rynn, Phys. Fluids 7, 284 (1964).
[7]G. J. Mullaney and N. R. Dibelius, ARSJ 31, 1575 (1961).
[8]G. E. Pikus, N. S. Skvortsov, and V. G. Yur'ev, Zh. Eksp. Teor. Fiz. 42, 330 (1962) [Sov. Phys.—JETP 15, 225 (1962)].
[9]M. N. Saha, Philos. Mag. 40, 472 (1920).
[10]L. Enriques and F. Magistrelli, Rev. Sci. Instru. 35, 1708 (1964).
[11]L. Agnew and C. Summers, Rev. Sci. Instru. 37, 1224 (1966).
[12]See Ref. 3, p. 292.
[13]J. C. Crown and A. Russek, Phys. Rev. 138, A669 (1965).
[14]B. J. Eastlund, J. Nucl. Energy C 8, 31 (1966).
[15]E. W. McDaniel, *Collision Phenomena in Ionized Gases* (Wiley, New York, 1964), p. 443.